Radiation Physics and Chemistry 171 (2020) 108746

Contents lists available at ScienceDirect

Radiation Physics and Chemistry

journal homepage: www.elsevier.com/locate/radphyschem

# Characterization of an extrapolation chamber in beta radiation beams and Monte Carlo modelling

Ivón Oramas Polo[a,*], William Souza Santos[a,b], Linda V.E. Caldas[a]

[a] Instituto de Pesquisas Energéticas e Nucleares, Comissão Nacional de Energia Nuclear, IPEN/CNEN, Av. Prof. Lineu Prestes, 2242, 05508-000, São Paulo, SP, Brazil
[b] Universidade Federal de Uberlândia, Instituto de Física, Av. João Naves de Ávila, 2121, Santa Mônica, 38400-902, Uberlândia, MG, Brazil

ARTICLE INFO

*Keywords:*
Extrapolation chamber
Beta radiation
BSS2
Monte Carlo

ABSTRACT

At the Calibration Laboratory (LCI) of the IPEN/CNEN, studies are in development on the establishment of a standard composed by the beta radiation sources for the dosimetry and calibration for personal monitoring in Brazil. For this purpose is used the Böhm extrapolation chamber (PTW model 23392). This chamber was already characterized at LCI in $^{90}Sr/^{90}Y$ beams using two different entrance windows: one of aluminized Mylar and another of PET (polyethylene terephthalate) known as Hostaphan. In this work, this extrapolation chamber was characterized in $^{85}Kr$ and $^{147}Pm$ beams. All tests were carried out with the reference $^{90}Sr/^{90}Y$ source, for comparison purposes. The Monte Carlo code MCNP5 code was used to obtain an extrapolation chamber and the BSS2 system sources computational model, based on the determination of the absorbed dose rate. Saturation curves, ion collection efficiency, ion recombination, polarity effect, stability of response, null depth, linearity of response, variation of response as a function of source-detector distance, extrapolation curves, correction factors and absorbed dose rates were obtained. The difference between the experimental absorbed dose rates and those obtained using the Monte Carlo model, compared to those from the calibration certificates, was less than 1.9% for the $10^8$ histories for each BSS2 system source. All results of the performed tests are within the limits of the international recommendations. The results for the $^{90}Sr/^{90}Y$ source were in good agreement with previous works performed at LCI. These results are suitable for the establishment of a standard instrument for the dosimetry and calibration of beta radiation sources and detectors in the LCI/IPEN. This standard will allow the calibration of detectors in beta radiation beams in dosimetry services in Brazil.

## 1. Introduction

The general objective of beta dosimetry is to provide information that helps to maintain the harmful effects of beta radiation within acceptable limits, and at large exposure events, that staff is assisted with appropriate medical treatments and prognoses (ICRU, 1997).

One of the main difficulties of determining the beta radiation dose is the large dose variation over short distances. The difficulty increases inside the tissue, due to the great attenuation of this radiation. Another difficulty is the need to measure doses in very thin layers such as the skin basal cells. To simulate these volumes, the detector must be extremely thin, with consequent reduction of sensitivity. These problems are further complicated by the large dispersion of beta radiation in air (ICRU, 1997).

The extrapolation chamber is the primary instrument established for the measurement of beta radiation (Böhm, 1986; Caldas, 1986; NIST, 2010; Behrens et al., 2011). The extrapolation chamber is a parallel-plate ionization chamber that has two parallel electrodes: the high voltage electrode or entrance window and the collecting electrode. The entrance window should be thin enough not to attenuate the beta radiation, but strong enough not to be deformed due to the applied voltage between it and the collecting electrode. To avoid the leakage current, and to define the volume inside the chamber, the collecting electrode is surrounded by a guard ring. Between the collecting electrode and the guard ring, an insulating material is used (Knoll, 2004).

The Böhm extrapolation chamber PTW model 23392 has been characterized in beta radiation beams in several works (Böhm, 1986; Behrens et al., 2011; Bakshi et al., 2013; Antonio et al., 2014; Reynaldo, 2015). However, the environmental conditions of temperature, pressure and relative humidity, as well as the radiation scattering differ from one laboratory to other. At the Calibration Laboratory (LCI/IPEN), a Böhm extrapolation chamber was characterized in $^{90}Sr/^{90}Y$ beta radiation source with the Beta Secondary Standard systems BSS1 and BSS2. In addition, two of the main characteristics of beta radiation sources were

* Corresponding author.
*E-mail addresses:* ivonoramas67@gmail.com (I.O. Polo), williathan@yahoo.com.br (W.S. Santos), lcaldas@ipen.br (L.V.E. Caldas).

https://doi.org/10.1016/j.radphyschem.2020.108746
Received 1 July 2019; Received in revised form 23 January 2020; Accepted 1 February 2020
Available online 04 February 2020
0969-806X/ 

determined: transmission factors and absorbed dose rates with two different entrance windows. The extrapolation chamber was established as the beta primary standard system in the calibration of detectors and sources of beta radiation for this source (Antonio et al., 2014).

The absorbed dose rate is the quantity established for beta radiation measurements (Böhm, 1986; Caldas, 1986). This quantity has been determined by the Monte Carlo (MC) method and then compared with experimental measurements (Behrens, 2013; Vahabi et al., 2014; Selvam et al., 2005; Faria et al., 2015; Polo et al., 2017, Polo et al., 2018a). The MC method allows the evaluation of the detectors and the equipment responses used in dosimetry. The MC method contributes to a better understanding of the radiation transport physics because of the potential to evaluate the different types of interactions, as well as to determine the different types of dosimetric quantities and correction factors for the radiation measurements (Andreo et al., 2017). An MC model of the extrapolation chamber and the BSS2 system sources allows to obtain physical parameters that are impossible or difficult to measure in practice. Examples of those parameters are: particle fluence, beta radiation correction factors and angular dependence (Polo et al., 2018b, Polo et al., 2019).

The objective of this work was to characterize the Böhm extrapolation chamber PTW model 23392 for the establishment of a standard composed of the $^{85}$Kr and $^{147}$Pm beta sources for the dosimetry and calibration of beta radiation sources and detectors in the LCI/IPEN. This standard will allow the calibration of beta radiation detector of dosimetry services in Brazil. Several tests were carried out to characterize the response of the extrapolation chamber. As a result of this work, a MC model for the extrapolation chamber and the BSS2 sources based on the determination of the absorbed dose rate was established. The default parameter ESTEP was modified to improve the differences between the Monte Carlo calculation and the experimental values and those from the calibration certificates.

## 2. Materials and methods

In this work, a commercial extrapolation chamber according to Böhm, PTW model 23392, of the LCI/IPEN was used. It has a graphite coated Mylar entrance window and collecting electrode of PMMA with graphite coated surface (PTW, 2002). A Keithley model 6517 B electrometer was used for the measurements with this extrapolation chamber.

The BSS2 sources were utilized for the development of this work. Table 1 shows the main characteristics of these sources (BSS2, 2005; PTB, 2005a, PTB, 2005b; PTB, 2005c).

In the BSS2 system, for use of the $^{85}$Kr and the $^{147}$Pm sources, a Hostaphan beam flattening filter must be used. For the $^{90}$Sr/$^{90}$Y source, the source-detector calibration distance of 11 cm was used without the beam flattening filter (BSS2, 2005).

In this work, the acceptance limits of the tests to evaluate the extrapolation chamber response will be those recommended by the International Electrotechnical Commission (IEC, 2011). This standard is recommended for dosimeters and ionization chambers used in radiotherapy.

**Table 1**
Main characteristics of the BSS2 beta sources.

| Characteristic | Radionuclide | | |
|---|---|---|---|
| | $^{147}$Pm | $^{85}$Kr | $^{90}$Sr/$^{90}$Y |
| Nominal activity | 3.7 GBq | 3.7 GBq | 460 MBq |
| Mean beta energy (MeV) | 0.06 | 0.24 | 0.8 |
| Calibration distance (cm) | 20 | 30 | 11, 20, 30, 50 |
| Calibration date | November 19, 2004 | November 30, 2004 | November 19, 2004 |
| Approximate half-life (days) | 958 | 3915 | 10483 |

As the voltage differences between the electrodes of an ionization chamber exposed to radiation increase from zero to a higher value, the collected current first increases almost linearly with the voltage and then increases more slowly, until it finally approaches asymptotically the saturation current for a given radiation intensity. The ionization current can be measured if all the ions formed in the chamber due to radiation reach the collecting electrode. The voltage versus current curve is called the saturation curve (Knoll, 2004). To obtain the saturation current and the efficiency of the chamber, a graph of the ionization current versus the inverse of the square root of the applied voltage is used. The obtained line is extrapolated to zero, thus obtaining the value of the saturation current (Dias and Caldas, 1999).

The ion collection efficiency of an ionization chamber is defined as the ratio of the measured current and the ideal saturation current. The ion collection efficiency can be determined by Equation (1) (Caldas, 1986; Dias and Caldas, 1999; Antonio et al., 2014):

$$f = I/I_s \tag{1}$$

The ion recombination losses can be determined by Equation (2) (Caldas, 1980):

$$f_r = 100 - f \tag{2}$$

The “polarity effect” is caused by negative current due to electrons that diffuse out of the backscattering material (Böhm, 1986). To estimate the polarity effect, Equation (3) is used:

$$k_{pol} = (I_- - I_+)/(I_- + I_+) \tag{3}$$

where $I_-$ and $I_+$ are the ionization currents measured at the negative and positive polarities, respectively.

The ionization current shall be multiplied by Equation (4) to correct the air density to the environmental reference conditions (Böhm, 1986):

$$k_{T,P} = P_0 * T/P * T_0 \tag{4}$$

The reference conditions are $T_0 = 293.15$ K and $P_0 = 101.3$ kPa.

To verify the stability of an ionization chamber response, it is necessary to perform the stabilization time test. According to the recommendations, the variation in the response of the currents measured at 15 min and 2 h later should not differ from 0.5% of the measured value after 1 h (IEC, 2011).

To evaluate the stability of the ionization chamber response, two tests are performed: repeatability test (short-term stability) and reproducibility test (long-term stability). The repeatability test is performed by taking 10 successive measurements with the ionization chamber and the control source. To evaluate the reproducibility of the ionization chamber, some repeatability tests are performed at a certain time. According to IEC (2011), the acceptance limit for the first test is 0.3% and 0.5% for the second one.

In order to verify the response of the ionization chamber as a function of the dose, the linearity of the response test is performed. The correlation coefficient of the linear fitting of the curves response should be as close as possible to 1.

In order to verify the inverse square law of the ionization chamber in beta radiation beams, the test of the variation of the chamber response in function of the source-detector distance is carried out.

To determine the absorbed dose rate in air and in tissue with an extrapolation chamber it is necessary to determine some parameters which are described as follows:

The ionization current in the sensitive chamber volume is calculated by Equation (5):

$$I = (I_+ - I_-)/2 \tag{5}$$

The minimum distance between the collecting electrode and the entrance window is known as the real null depth. The extrapolation chambers are constructed with this safety so that the electrodes do not

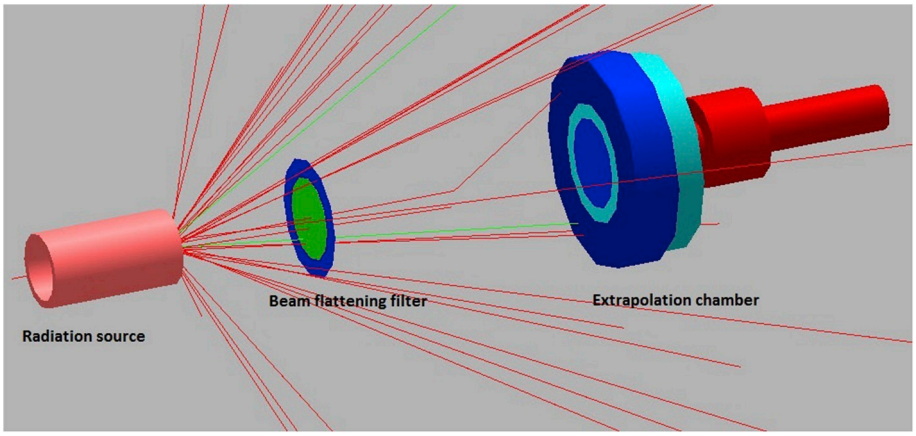


**Fig. 1.** Monte Carlo model of the extrapolation chamber, $^{85}$Kr radiation source and beam flattening filter.

touch each other. The real null depth can be determined from the extrapolation of the straight lines of the ionization current as a function of the depth of the extrapolation chamber for both polarities. The absolute value of the point of meeting of the lines corresponds to the real null depth (Caldas, 1986).

The behavior of the ionization current of an extrapolation chamber as a function of depth is represented by the extrapolation curve. To obtain this curve, the sensitive volume of the chamber must be varied (Böhm, 1986).

To determine the absorbed dose rate in the tissue with an extrapolation chamber, the Equation (6) from (ISO, 2004) is used:

$$\dot{D}_{\beta} = \frac{\left(\bar{W}_0/_e\right) s_{t,a}}{\rho_{a0} * a}\left[\frac{d}{dl}\{kk`I(l)\}\right] l = 0 \tag{6}$$

where

$\left(\bar{W}_0/_e\right)$ is the quotient of the mean energy to produce an ion pair in air under reference conditions and the elementary charge;
$s_{t,a}$ is the quotient of mass-electronic stopping powers of tissue and air;
$\rho_{a0} = 1.1974 kg/m^3$ is the density of air at reference conditions which are defined for the parameters: ambient temperature $T_0$, atmospheric pressure $p_0$ and relative humidity $r_0 = 0.65$;
$a$ is the effective area of the extrapolation chamber collecting electrode;
$I(l)$ is the ionization current;
$\left[\frac{d}{dl}\{kk'I(l)\}\right] l = 0$ is the limiting slope value for $l=0$ of the corrected ionization current versus chamber depth.

Because Bragg-Gray conditions are not achieved in beta radiation measurements, it is necessary to determine several correction factors (ISO, 2004). The correction factors are the following:

$k$ is the product of the correction factors which are dependent on the chamber depth or some other varying parameters, consisting of the following correction factors:
$k_{ac}$ for attenuation of beta-particles in the collecting volume;
$k_{ad}$ for air density in the collecting volume;
$k_{abs}$ for attenuation and scattering of beta-particles between the source and the collecting volume;
$k_{de}$ for radioactive decay, $k_{di}$ for axial non-uniformity;
$k_{pe}$ for perturbation of the beta-particle flux density by the side walls of the extrapolation chamber;
$k_{sat}$ for ionization collection losses due to ion recombination.
$k'$ is the product of correction factors which are independent of the chamber depth or are constant during the measurement. They consist of the following correction factors:
$k_{ba}$ for backscattering from the collecting electrode and guard ring;
$k_{br}$ for Bremsstrahlung from the beta-particle source;
$k_{el}$ for electrostatic attraction of the entrance window;
$k_{hu}$ for the effect due to variations of the relative air humidity;
$k_{in}$ for interface effects;
$k_{ra}$ for radial non-uniformity.

The correction factors $k$ and $k'$ were determined according to Böhm (1986) and ISO 6980–2:2004 report (ISO, 2004). *The correction factors $k_{br}$ and $k_{ba}$* were determined by the Monte Carlo method (Polo et al., 2018b).

The MCNP5 is a MC particle transport code that includes the MCNP5 and the MCNPX 2.6.0 data libraries. The code was developed by Los Alamos National Laboratory, and it can be used for neutrons, photons, electrons, or coupled neutrons /photons /electrons transport. With the MCNP5 code, the user can create a geometry based on a three-dimensional configuration of the materials of the physical problem with geometric cells delimited by surfaces of different types (MCNP, 2008; Kirk, 2010).

The MC model previously reported for the extrapolation chamber was used for all simulations (Polo et al., 2018b). The following material densities used in the simulations for Al, steel, Ti, $Pm_2O_3$, Ag, Kr, $SrCO_3$ and air were 2.85, 8.06, 4.4, 6.85, 10.5, 0.0191, 3.76 and $1.1974 \times 10^{-3}$ g/cm$^3$, respectively (ICRU, 1997). For the simulation, the null depth of the extrapolation chamber of $(0.102 \pm 0.021)$ mm was considered. The nominal activities of the radiation sources and the source-detector distances considered are shown in Table 1. For the $^{90}$Sr/$^{90}$Y source, the source-detector calibration distance of 11 cm was considered without the beam flattening filter. The actual dimensions of the sources, including their shielding, were considered. The $^{90}$Sr/$^{90}$Y source is distributed in the form of carbonate in a silver substrate, the $^{85}$Kr source is gaseous, and the $^{147}$Pm is distributed as $Pm_2O_3$. Fig. 1 shows the MCNP5 model of the extrapolation chamber and the $^{85}$Kr radiation source (Vised version X_22 S).

For the determination of the absorbed dose rate, the procedure used in a previous work was followed (Polo et al., 2018a). According to Andreo et al. (2017), the absorbed dose rate was calculated by the Equation (7):

$$\dot{D} = A * \bar{E} * \left(\frac{\text{MeV}}{\text{g. s}}\right) * 1{,}60 * 10^{-13} * \left(\frac{\text{J}}{\text{MeV}}\right) * 10^{3}\left(\frac{\text{g}}{\text{kg}}\right) = 1{,}60 * 10^{-10} * A * \bar{E}\left(\frac{\text{Gy}}{\text{s}}\right) \tag{7}$$

where $A$ is the source activity in Bq and $\bar{E}$ is the mean energy in MeV per disintegration.

The absorbed dose rate in the tissue $(\dot{D}_t)$ in the sensitive volume of the extrapolation chamber was calculated by Equation (8) (ISO, 2004):

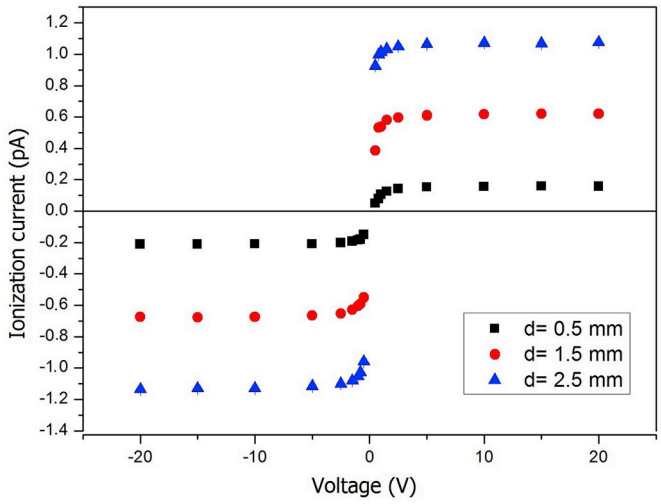


**Fig. 2.** Saturation curves of the extrapolation chamber for the $^{85}$Kr source (d- Chamber depth).

$$\dot{D}_t = \dot{D} * s_{t,a} \quad (8)$$

The tally *F8 (energy deposition) was used.

## 3. Results and discussion

### 3.1. Saturation curves

The saturation curves of $^{90}$Sr/$^{90}$Y and $^{85}$Kr sources were obtained at source-detector distances of 11 cm and 30 cm, respectively. The experiment performed with the $^{147}$Pm source did not present an adequate signal to carry out the complete study. The polarization voltage was varied between −20 V and +20 V. The saturation curves of the ionization current corresponding to the $^{85}$Kr source are shown in Fig. 2. The graphs corresponding to the saturation ionization current obtained by the extrapolation procedure to zero of the ionization current are shown in Fig. 3.

In Table 2, the values of the saturation current for the 0.5 mm, 1.5 mm and 2.5 mm chamber depths, the ion collection efficiency, the ion recombination and the polarity effect are shown. These values correspond to the $^{90}$Sr/$^{90}$Y and $^{85}$Kr sources.

The results obtained may be considered acceptable. The extrapolation chamber response presented a collection efficiency above 99%, which is the limit recommended by IEC (2011). The results

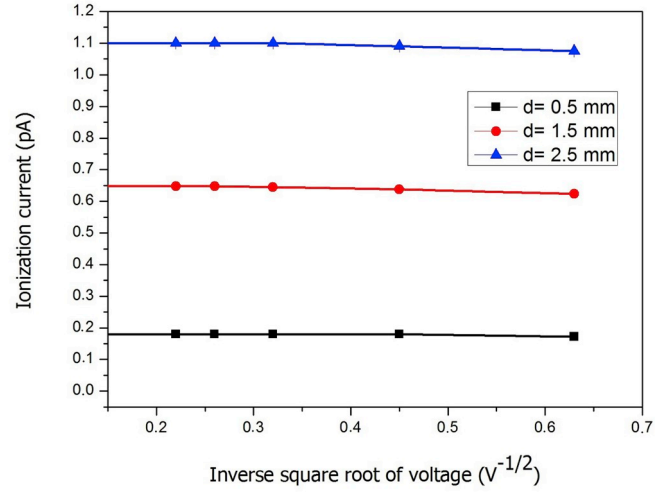


**Fig. 3.** Saturation currents for the $^{85}$Kr source (d- Chamber depth).

demonstrated that the ion collection efficiency increases with the increasing depth and the increased bias voltage. The results are in agreement with those reported by Caldas (1980) and Antonio et al. (2014).

The effects of ion recombination are important for small volumes. The determination of ion recombination losses can be considered acceptable since IEC (2011) recommends that this value should be less than 1%.

The effect of polarity decreased as the chamber depth increased. The IEC standard (2011) recommends a value of 1% for the polarity effect, but according to Antonio (2013), when it deals with beta radiation, there is an ionization current originated at the moment when beta particles interact with the material of the extrapolation chamber entrance window. This behavior was also reported by Böhm (1986), NIST (2010) and Antonio et al. (2014). Böhm (1986) and NIST (2010) obtained polarity effects higher than 10%. Böhm, 1986 obtained a polarity effect up to 10%, NIST (2010) achieved a maximum value of 16%, and Antonio et al. (2014) obtained more than 19%. The polarity effect values can be considered acceptable because they are related to beta radiation.

### 3.2. Stabilization time

For the stabilization time test, the chamber was exposed to the $^{90}$Sr/$^{90}$Y source at a distance of 11 cm, a chamber depth of 2.5 cm and a voltage of ± 25 V. This voltage was applied to the chamber after intervals of 15 min, 1 h and 2 h according to the recommendations of the IEC (2011). The test was performed for both polarities and the ionization currents were normalized to the current value measured after 1 h. The results obtained for the stabilization time test are shown in Table 3.

The results obtained for both polarities are in good agreement with the IEC (2011) recommendation.

### 3.3. Stability of response

To verify the stability of the extrapolation chamber response, the tests of repeatability and reproducibility were performed. To perform these tests, the extrapolation chamber was positioned at 11 cm from the $^{90}$Sr/$^{90}$Y source. The established chamber depth was 2.5 mm and the applied voltage was ± 25 V. For the repeatability test, the electric charge collection time intervals were 10 s in 10 measurements. For the reproducibility test, measurements with the same parameters were repeated for 13 months.

According to IEC (2011), for the repeatability test, the coefficient of variation (CV) should not exceed 0.3% for series of 10 measurements, and for the reproducibility test, the CV should be ± 0.5% of the value taken as reference. The repeatability of the response presented a CV less than 0.15%. All measurements of the reproducibility test showed a CV less than 0.36%. Therefore, measurements were within the limits established by IEC (2011).

The results obtained in the reproducibility test are shown in Fig. 4.

### 3.4. Null depth

The null depth of the extrapolation chamber was obtained by the two polarities method (Caldas, 1980). The chamber was exposed to the radiation fields of the sources: $^{90}$Sr/$^{90}$Y at 11 cm without beam flattening filter, $^{85}$Kr at 30 cm with filter and $^{147}$ Pm at 20 cm with filter. In all cases, the chamber depth was varied from 0.5 mm to 2.5 mm in increments of 0.5 mm, and the applied voltage was from 5 V to 25 V for the positive and negative polarities.

The null depth was determined from the extrapolation of the linearly fitting lines of the ionization current plots as a function of the chamber depth for both polarities. The absolute value of the interception point was determined by the equations of the fitting lines. Table 4 shows the obtained values for all three sources with the coefficients of

**Table 2**
Saturation current for the 0.5 mm, 1.5 mm and 2.5 mm chamber depths, ion collection efficiency, ion recombination and polarity effect corresponding to the $^{90}Sr/^{90}Y$ and $^{85}Kr$ sources.

| Voltage (V) | Saturation current (pA) | Ion collection efficiency $f$ (%) | Ion recombination $f_r$ (%) | Polarity effect $k_{pol}$ (%) |
|---|---|---|---|---|
| | | $^{90}Sr/^{90}Y$ | | |
| | | Chamber depth 0.5 mm | | |
| 2.5 | 0.8466 ± 0.0005 | 97.2 | 2.8 | 33.1 |
| 5 | | 97.6 | 2.4 | 32.1 |
| 10 | | 98.3 | 1.7 | 32.8 |
| 15 | | 98.5 | 1.4 | 32.9 |
| 20 | | 98.9 | 1.1 | 32.6 |
| | | Chamber depth 1.5 mm | | |
| 2.5 | 2.9100 ± 0.0027 | 97.23 | 2.8 | 8.6 |
| 5 | | 99.4 | 0.6 | 9.3 |
| 10 | | 99.9 | 0.08 | 9.4 |
| 15 | | 99.9 | 0.07 | 9.5 |
| 20 | | 100 | 0.0 | 8.9 |
| | | Chamber depth 2.5 mm | | |
| 2.5 | 4.9800 ± 0.0018 | 97.5 | 2.5 | 5.3 |
| 5 | | 98.7 | 1.3 | 5.2 |
| 10 | | 99.4 | 0.6 | 5.3 |
| 15 | | 99.6 | 0.4 | 5.2 |
| 20 | | 99.6 | 0.4 | 5.2 |
| | | $^{85}Kr$ | | |
| | | Chamber depth 0.5 mm | | |
| 2.5 | 0.1820 ± 0.0004 | 94.6 | 5.4 | 17.0 |
| 5 | | 99.6 | 0.3 | 16.0 |
| 10 | | 100 | 0.0 | 15.0 |
| 15 | | 100 | 0.0 | 14.0 |
| 20 | | 100 | 0.0 | 14.0 |
| | | Chamber depth 1.5 mm | | |
| 2.5 | 0.65442 ± 0.0007 | 95.3 | 4.6 | 5.0 |
| 5 | | 97.5 | 2.5 | 4.0 |
| 10 | | 98.7 | 1.3 | 5.0 |
| 15 | | 99.04 | 0.9 | 4.0 |
| 20 | | 99.08 | 0.9 | 4.0 |
| | | Chamber depth 2.5 mm | | |
| 2.5 | 1.1010 ± 0.0005 | 97.7 | 2.3 | 2.4 |
| 5 | | 99.1 | 0.9 | 2.5 |
| 10 | | 100 | 0.0 | 2.7 |
| 15 | | 100 | 0.0 | 2.9 |
| 20 | | 100 | 0.0 | 2.7 |

**Table 3**
Stabilization time.

| Time (min) | Normalized ionization current for 60 min | |
|---|---|---|
| | Positive polarity | Negative polarity |
| 15 | 0.9989 ± 0.0007 | 0.9988 ± 0.0012 |
| 60 | 1.0000 ± 0.0007 | 1.0000 ± 0.0015 |
| 120 | 0.9993 ± 0.0012 | 0.9985 ± 0.0012 |

variation. In the case of the $^{147}Pm$ source, the value was $(-0.102 \pm 0.021)$ mm, but since the real null depth is an absolute value, it is positive.

Figs. 5 and 6 show the graphs for the determination of the null depth of the extrapolation chamber using the $^{90}Sr/^{90}Y$ and $^{85}Kr$ and sources. The graph for the $^{147}Pm$ source was reported before by Polo et al. (2018b). The results can be considered similar, taking into account the uncertainties of the values for each source.

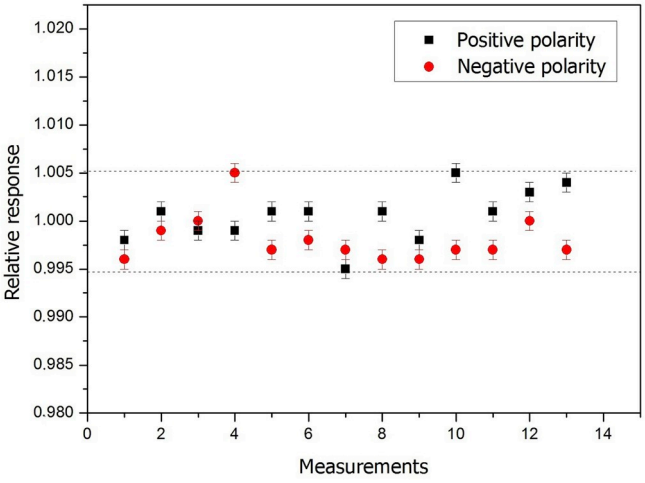


**Fig. 4.** Reproducibility of response of the extrapolation chamber.

### 3.5. Linearity of response

The linearity of the response of the extrapolation chamber was analyzed in relation to the electric charge as a function of the radiation dose. For the $^{90}Sr/^{90}Y$, $^{85}Kr$ and $^{147}Pm$ sources the doses were from 1 mGy to 8 mGy, from 1 mGy to 2.5 mGy and from 0.090 mGy to 0.486 mGy, respectively. The results and the ratios "electric charge/dose" are presented in Fig. 7. The coefficients of variation were less than 2.53%, 4.03% and 11.21% for the $^{90}Sr/^{90}Y$, $^{147}Pm$ and $^{85}Kr$ sources, respectively. The correlation coefficients of the $R^2$ linear adjustment were 1.0000, 0.9852 and 0.9999 for the previously mentioned sources. The ratios "electric charge/dose" in Fig. 7 confirm the good linearity of response of the absorbed dose for these sources in the tested dose range.

**Table 4**
Values of the null depth of the extrapolation chamber for the $^{90}Sr/^{90}Y$, $^{85}Kr$ and $^{147}Pm$ sources.

| Source | Null depth (mm) | Coefficient of variation (%) |
|---|---|---|
| $^{90}Sr/^{90}Y$ | 0.094 ± 0.001 | 1.51 |
| $^{85}Kr$ | 0.096 ± 0.009 | 8.9 |
| $^{147}Pm$ | 0.102 ± 0.021 | 20.3 |

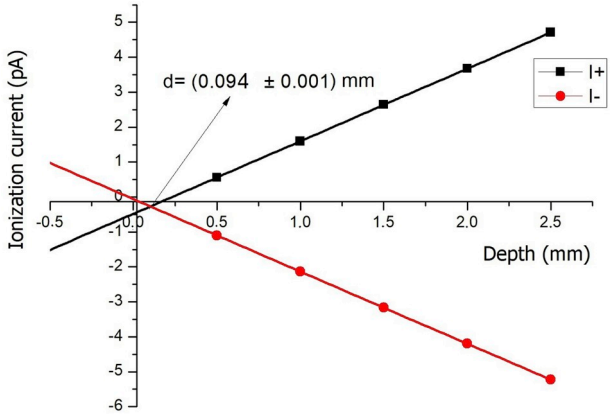


**Fig. 5.** Null depth of the extrapolation chamber for the $^{90}Sr/^{90}Y$ source.

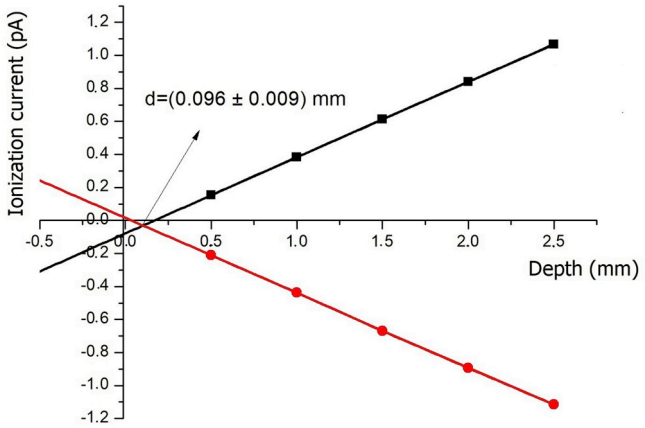


**Fig. 6.** Null depth of the extrapolation chamber for the $^{85}Kr$ source.

### 3.6. Variation of the extrapolation chamber response as a function of the source-detector distance

The extrapolation chamber was exposed to the $^{90}Sr/^{90}Y$ source to verify its response as a function of the source-detector distance. In this test, the applied voltage and the chamber depth were ± 25 V and 2.5 mm, respectively. The distance was varied from 11 cm to 50 cm. In Table 5 are shown the values of the ionization current determined from the currents of negative and positive polarities. The Table also shows the product of the ionization current by the square of distance $I_n * (d_n)^2$, and in the other column, is presented an equation to assess if the extrapolation chamber response follows the Inverse Square Law. The ionization current was determined from Equation (5).

The third and fourth columns of Table 5 clearly show that the extrapolation chamber presents a deviation from the Inverse Square Law.

### 3.7. Absorbed dose rates

The absorbed dose rates were determined for the $^{90}Sr/^{90}Y$, $^{85}Kr$ and $^{147}Pm$ sources at the source-detector distances of 11 cm, 30 cm and 20 cm respectively, according to the specifications of the calibration certificates of the sources (PTB, 2005a; PTB, 2005b; PTB, 2005c). The chamber depth and the voltage were varied from 0.5 mm to 2.5 mm and from ± 5 V to ± 25 V, respectively. This range of chamber depths was adopted because Böhm (1986) demonstrated that at greater depths occur significant deviations in determination of the correction factors. In addition, previous experiments showed that the range of chamber depth between 0.5 mm to 2.5 mm is enough to obtain all the extrapolation curves (Caldas, 1980).

The absorbed dose rate in the air and in the tissue were determined using Equations (7) and (8) respectively.

The quantities used to determine the absorbed dose rate in the tissue were as follows: $\bar{W}_o/e$= (33.83 ± 0.06) (J/C), $\rho_{a0}$= (1.1974 ± 0.0005) (kg/m$^3$) (ISO, 2004). The quotient of mass-electronic stopping powers of tissue and air are 1.110, 1.121 and 1.124 for the $^{90}Sr/^{90}Y$, $^{85}Kr$ and $^{147}Pm$ sources, respectively. The values and uncertainties presented are in agreement with Böhm (1986) and ISO (2004). The determination of the effective area of the collecting electrode was performed by Antonio et al. (2014) using a mechanical method. The area of the collecting electrode of the extrapolation chamber obtained was (735.41 ± 0.24) mm$^2$.

The correction factors to determine the absorbed dose rate in the tissue and their uncertainties were determined according to the recommendations (Böhm, 1986; ISO, 2004).

The extrapolation curves for all sources were determined by taking measurements of the ionization current for each chamber depth. The measured currents were corrected by Equation (4). The depths were corrected taking into account the real null depth of the extrapolation chamber. Fig. 8 shows the extrapolation curves obtained for the $^{90}Sr/^{90}Y$, $^{85}Kr$ and $^{147}Pm$ sources and the ratios "ionization current /corrected chamber depth". The correlation coefficients of the linearly fitting curves were: 0.99992, 0.99999 and 0.99167 respectively.

The angular coefficient of each curve was determined by the fitting of the extrapolation curves for each source. The angular coefficients were as follows: (2.932 ± 0.025) pA/m, (1.071 ± 0.011) pA/m and (0.299 ± 0.005) pA/m for the $^{90}Sr/^{90}Y$, $^{85}Kr$ and $^{147}Pm$ sources, respectively. The measurements resulted with very low uncertainties, not visible in the graphics.

The absorbed dose rates in air and tissue at zero depth (at the surface of the chamber window) were determined for all 3 sources. Table 6 shows the values and the uncertainties of the absorbed dose rates in air at the null depth for each source, and the values of the calibration certificates for the indicated calibration distances (PTB, 2005a; PTB, 2005b; PTB, 2005c).

Table 7 shows the values and the uncertainties of the absorbed dose rates in tissue at the null depth for each source, and the values of the calibration certificate for the calibration distances (PTB, 2005a; PTB, 2005b; PTB, 2005c) at the indicated depth.

Table 8 shows the values and the uncertainties of the absorbed dose rates in air at the depth of 0.07 mm for each source, and the values of the calibration certificates for the indicated calibration distances (PTB, 2005a; PTB, 2005b; PTB, 2005c).

Table 9 shows the values and the uncertainties of the absorbed dose rates in tissue at the depth of 0.07 mm for each source, and the values of the calibration certificates for the indicated calibration distance (PTB, 2005a; PTB, 2005b; PTB, 2005c).

The source calibration certificates present the absorbed dose rate to 0.07 mm depth in the tissue. In this work, the absorbed dose rates in tissue at null depth were determined, and the values of the calibration certificate were converted to this magnitude for comparative purposes. The differences between the values obtained and those of the source calibration certificate could be given by the activity of the sources and all the uncertainties resulting from the measurements.

Bakshi et al. (2013) presented differences between the absorbed dose rates in air and the certificates of 1.22%, 0.10% and 1.27% for $^{90}Sr/^{90}Y$, $^{85}Kr$ and $^{147}Pm$ sources of the BSS2 system of Radiological Physics & Advisory Division (RP & AD) of Bhabha Atomic Research Centre, India.

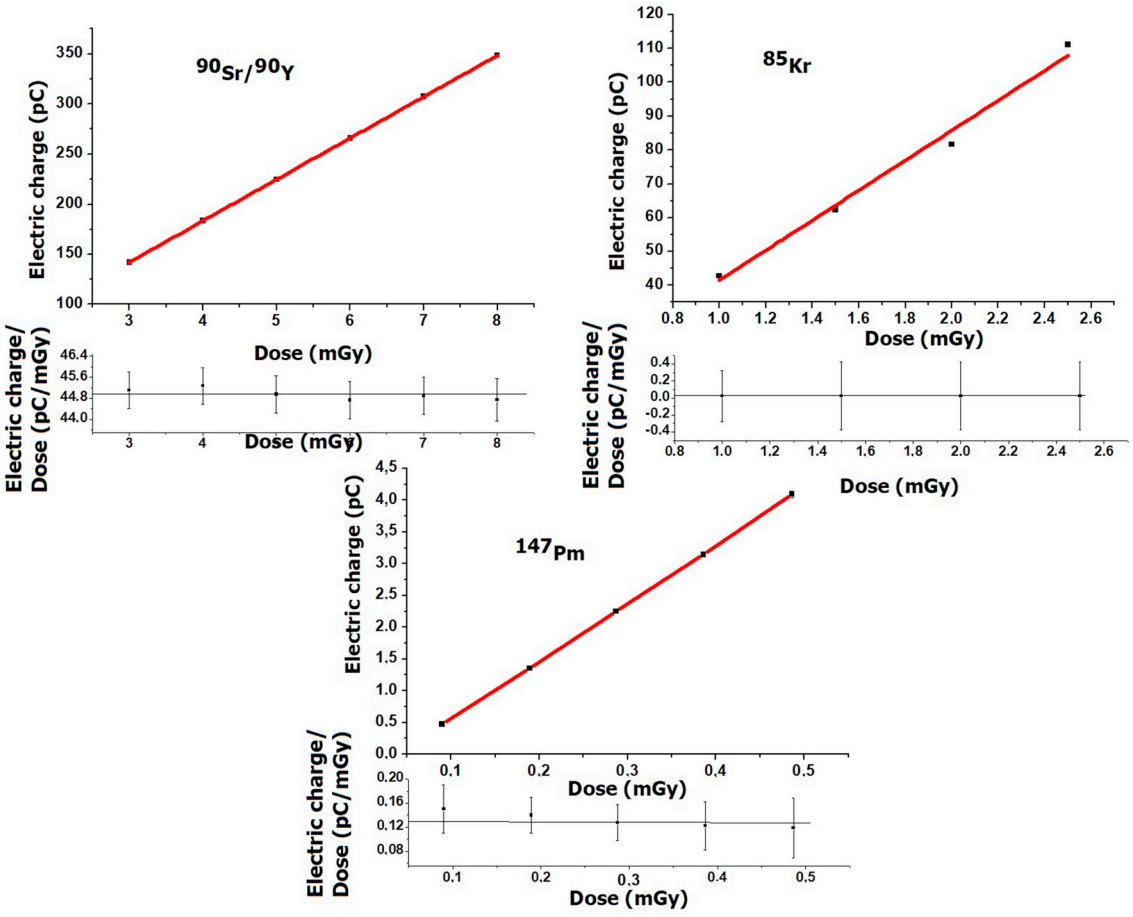


**Fig. 7.** The linearity of response as a function of the absorbed dose for the $^{90}Sr/^{90}Y$, $^{85}Kr$ and $^{147}Pm$ sources.

**Table 5**
Ionization current as a function of the source-detector distance ($I_n$-ionization current, $d_3$-source-detector distance at 50 cm, $d_n$-source-detector distances at 11 cm, 20 cm and 30 cm).

| Source-detector distance (cm) | Ionization current (pA) | $I_n * (d_n)^2$ (pA*cm$^2$) | $I_n*(d_n)^2/I_3*(d_3)^2$ |
|---|---|---|---|
| 11 | 4.9675 ± 0.0020 | 601.07 | 0.948 |
| 20 | 1.5698 ± 0.0022 | 627.9 | 0.990 |
| 30 | 0.7043 ± 0.0016 | 633.9 | 1.000 |
| 50 | 0.2536 ± 0.0015 | 634.0 | 1.000 |

The obtained results are considered acceptable considering that they are within the uncertainties and taking into account the comparisons with previous works.

### 3.8. Absorbed dose rates determined by the Monte Carlo method

A MC model of the extrapolation chamber and the BSS2 system sources was created with the MCNP5 code.

The initial number of histories for the simulation of each source was $10^8$. For electron transport, the Integrated TIGER Series electron physics (ITS) mode was used. The statistical tests carried out by the MCNP were fulfilled (MCNP, 2008). Material data were created using the recommendation of ICRU 90 (2016).

According to literature Lee et al. (2018) and Zoros et al. (2014), it is possible to improve the accuracy of dosimetric calculation in MCNP by changing the transport parameters applied to the simulations with condensed history algorithms. To achieve this objective the value of the MCNP ESTEP parameter can be modified. Lee et al. (2018) showed that

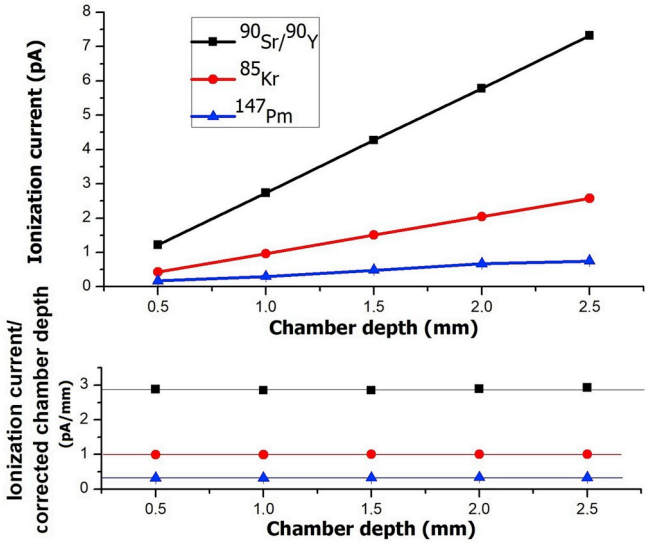


**Fig. 8.** Extrapolation curves for the $^{90}Sr/^{90}Y$, $^{85}Kr$ and $^{147}Pm$ sources.

the result of Fano is affected by the value of the ESTEP parameter. The default ESTEP parameter is 3. To reduce the differences between the Monte Carlo calculation and the experimental values and those from calibration certificate the ESTEP parameter was set to 80.

Table 10 shows a comparison among the values of absorbed dose rates of the MCNP model, the experimentally and the absorbed dose rates from the calibration certificates.

**Table 6**
Absorbed dose rates in air at null depth determined experimentally for each source and values of the calibration certificates.

| Source | Source-detector distance (cm) | Absorbed dose rate in air at null depth (μGy/s) | Absorbed dose rate in air from PTB certificate at null depth (μGy/s) | Difference (%) |
|---|---|---|---|---|
| $^{90}Sr/^{90}Y$ | 11 | 113.4 ± 2.2 | 111.1 ± 1.9 | 2.07 |
| $^{85}Kr$ | 30 | 41.65 ± 1.06 | 41.7 ± 0.7 | 0.12 |
| $^{147}Pm$ | 20 | 11.5 ± 0.5 | 11.37 ± 0.29 | 1.14 |

**Table 7**
Absorbed dose rates in tissue at null depth determined experimentally for each source and values of the calibration certificates.

| Source | Source - detector distance (cm) | Absorbed dose rate in tissue at null depth (μGy/s) | Absorbed dose rate in tissue from PTB certificate at null depth (μGy/s) | Difference (%) |
|---|---|---|---|---|
| $^{90}Sr/^{90}Y$ | 11 | 125.9 ± 2.9 | 123.32 ± 2.06 | 2.09 |
| $^{85}Kr$ | 30 | 46.69 ± 1.20 | 46.7 ± 0.8 | 0.02 |
| $^{147}Pm$ | 20 | 12.9 ± 0.5 | 12.8 ± 0.3 | 0.8 |

**Table 8**
Absorbed dose rates in air at the depth of 0.07 mm determined experimentally for each source and values of the calibration certificates.

| Source | Source- detector distance (cm) | Absorbed dose rate in air at the depth of 0.07 mm (μGy/s) | Absorbed dose rate in air from certificate at the depth of 0.07 mm (μGy/s) | Difference (%) |
|---|---|---|---|---|
| $^{90}Sr/^{90}Y$ | 11 | 118.30 ± 2.13 | 119.5 ± 1.5 | 1.00 |
| $^{85}Kr$ | 30 | 39.5 ± 1.4 | 39.7 ± 0.5 | 0.5 |
| $^{147}Pm$ | 20 | 2.41 ± 3.22 | 2.35 ± 0.05 | 2.5 |

**Table 9**
Absorbed dose rates in tissue at the depth of 0.07 mm determined experimentally for each source and values of the calibration certificates.

| Source | Source- detector distance (cm) | Absorbed dose rate in tissue at the depth of 0.07 mm (μGy/s) | Absorbed dose rate in tissue from certificate at the depth of 0.07 mm (μGy/s) | Difference (%) |
|---|---|---|---|---|
| $^{90}Sr/^{90}Y$ | 11 | 131.3 ± 4.3 | 132.6 ± 1.7 | 0.98 |
| $^{85}Kr$ | 30 | 44.2 ± 2.8 | 44.5 ± 0.6 | 0.67 |
| $^{147}Pm$ | 20 | 2.7 ± 3.6 | 2.64 ± 0.06 | 2.27 |

**Table 10**
Absorbed dose rates in tissue simulated by the Monte Carlo code, experimental results and the values from the PTB calibration certificates.

| Absorbed dose rate (μGy/s) | Source | | |
|---|---|---|---|
| | $^{90}Sr/^{90}Y$ | $^{85}Kr$ | $^{147}Pm$ |
| Calibration certificade (A) | 123.32 ± 2.06 | 46.7 ± 0.8 | 12.8 ± 0.3 |
| Experimental results (B) | 125.9 ± 2.9 | 46.69 ± 1.20 | 12.9 ± 0.5 |
| Monte Carlo code (C) | 123.5 ± 0.6 | 46.24 ± 1.03 | 12.7 ± 1.8 |
| Difference between A and C (%) | 0.14 | 0.98 | 0.8 |
| Difference between B and C (%) | 1.9 | 0.96 | 1.6 |

The uncertainties of the MC estimated dose rate reflect the number of simulated histories. Several simulations were made to reach these uncertainty values. The difference between the absorbed dose rates for the three sources was less than 1.9%. Faria et al. (2015) presented results of 1.56%, 4.7% and 3.96% for the differences between the absorbed doses rates of the calibration certificates and the dose rates determined by the MCNP MC code for the $^{90}Sr/^{90}Y$, $^{85}Kr$ and $^{147}Pm$ sources respectively.

## 4. Conclusions

The characterization of the Böhm extrapolation chamber model 23392 in $^{85}Kr$ and $^{147}Pm$ beta radiation beams was performed. Several tests were carried out: saturation curves, ion collection efficiency, ion recombination, polarity effect, stability of response, stabilization time, null depth, linearity of response, variation of response as a function of source-detector distance and extrapolation curves. The correction factors for beta radiation and absorbed dose rates in air and in tissue were obtained. Moreover, a Monte Carlo MCNP5 model for the extrapolation chamber and the BSS2 sources was established for the comparison of the absorbed dose rate. All tests, including the Monte Carlo model, were performed for the $^{90}Sr/^{90}Y$ source at the distance of 11 cm, because it is the reference source for beta radiation. All tests performed showed agreement with the international recommendations.

The agreement of the characterization tests and the Monte Carlo model are suitable for the establishment of a standard composed of the cited beta sources for the dosimetry and calibration of beta radiation sources and detectors in the LCI/IPEN. This standard can be used in the calibration of dosimeters for personal monitoring in all services in Brazil.

## CRediT authorship contribution statement

**Ivón Oramas Polo:** Conceptualization, Methodology, Software, Validation, Formal analysis, Investigation, Writing - original draft, Writing - review & editing. **William Souza Santos:** Software, Validation, Methodology, Data curation. **Linda V.E. Caldas:** Conceptualization, Methodology, Supervision, Validation, Writing - review & editing.

## Declaration of competing interest

The authors declare that they have no known competing financial interests or personal relationships that could have appeared to influence the work reported in this paper.

## Acknowledgments

The authors thank the partial financial support of the Brazilian funding agencies CNPq (Processes: 142297/2015-1 fellowship of I.O. Polo, and 301335/2016-8) and CAPES (Project: 554/2018).

## References

Andreo, P., Burns, D.T., Nahum, A.E., Seuntjens, J., Attix, F.H., 2017. Fundamentals of Ionizing Radiation Dosimetry. Wiley-VCH Verlag GmbH & Co., Weinheim, Germany.

Antonio, P.L., 2013. Establishment of Primary Standardization and Relative Methodswith the use of Luminescent Techniques in Beta Radiation Dosimetry. São Paulo (Ph.D.Thesis). Energy Nuclear and Research Institute (IPEN/CNEN), São Paulo, Brazil (In Portuguese).

Antonio, P.L., Xavier, M., Caldas, L.V.E., 2014. Böhm extrapolation chamber: study of its behavior in beta radiation fields at the Calibration Laboratory of IPEN. Radiat. Phys. Chem. 104, 310–315.

Bakshi, A.K., Vandana, S., Palani Selvam, T., Chougaonkar, M.P., Mayya, Y.S., 2013. Measurement of the output of ISO recommended beta sources with an extrapolation chamber. Radiat. Meas. 53–54, 50–55.

Behrens, R., Fedina, S., Oborin, A., 2011. Direct comparison of extrapolation chamber measurements of the absorbed dose rate for beta radiation between PTB (Germany) and VNIIM (Russia). Metrologia 48, 317–323.

Behrens, R., 2013. Simulation of the radiation fields of the beta secondary standard BSS2. J. Instr. 8, P02019.

Böhm, J., 1986. The National Primary Standard of the PTB for realizing the Unit of the Absorbed Dose Rate to Tissue for Beta Radiation. Physikalisch-Technische Bundesanstalt, PTB-Dos-13, Braunschweig, Germany. https://oar.ptb.de/resources/show/10.7795/110.20190315A.

BSS2, 2005. Beta Secondary Standard 2. Operation Manual. QSA Global GmbH, Germany.

Caldas, L.V.E., 1980. Some Calibration and Dosimetry Methods for Beta Radiation. Ph.D.Thesis. Physics Institute/São Paulo University, São Paulo, Brazil (In Portuguese).

Caldas, L.V.E., 1986. Performance characteristics of an extrapolation chamber for beta radiation detection. Appl. Radiat. Isot. 37 (9), 988–990.

Dias, S.K., Caldas, L.V.E., 1999. Characteristics of an extrapolation chamber for β-ray protection level measurements. J. Appl. Phys. 86 (1), 671–673.

Faria, F.P., Reynaldo, S., Fonseca, T.C.F., Lacerda, M.A.S., Da Silva, T.A., 2015. Monte Carlo simulation applied to the characterization of an extrapolation chamber for beta radiation dosimetry. Radiat. Phys. Chem. 116, 226–230.

ICRU, 1997. International Commission on Radiation Units and Measurements. Dosimetry of External Beta Rays for Radiation Protection 56 ICRU Report, Bethesda.

ICRU, 2016. Key Data for Ionizing-Radiation Dosimetry: Measurement Standards and Applications. J. ICRU 14 ICRU Report 90.

IEC, 2011. International Electrotechnical Commission. Medical Electrical Equipment Dosimeters with Ionization Chambers as used in Radiotherapy. IEC, Geneve, pp. 60731.

ISO, 2004. International Organization for Standardization. Nuclear Energy – Reference Beta-Particle Radiation – Part 2: Calibration Fundamentals related to Basic Quantities characterizing the Radiation Fields. ISO, 2004 (ISO 6980-2:2004), Genève.

Kirk, B.L., 2010. Overview of Monte Carlo radiation transport codes. Radiat. Meas. 45, 1318–1322.

Knoll, G., 2004. Radiation Detection and Measurement. John Wiley and Sons, New York.

Lee, J., Lee, J., Ryu, D., Lee, H., Ye, S.J., 2018. Fano cavity test for electron Monte Carlo transport algorithms in magnetic fields: comparison between EGSnrc, PENELOPE, MCNP6 and Geant4. Phys. Med. Biol. 63, 195013.

MCNP, 2008. MCNP: A General Monte Carlo N-Particle Transport Code, Version 5, Volume I: Overview and Theory, LA-UR-03-1987. Los Alamos National Laboratory.

NIST, 2010. National Institute of Standards and Technology. Ionizing Radiation Division: Protection-level Beta Particle Source & Instrument Calibrations. IRD-P-10. pp. 1–39.

Polo, I.O., Souza, W.S., Antonio, P.L., Caldas, L.V.E., 2017. Variance reduction technique in a beta radiation beam using an extrapolation chamber. Appl. Radiat. Isot. 128, 154–157.

Polo, I.O., Souza, W.S., Caldas, L.V.E., 2018a. Modelling the absorbed dose rate of the beta standard BSS2 $^{147}$Pm source. Appl. Radiat. Isot. 140 86–86.

Polo, I.O., Souza, W.S., Caldas, L.V.E., 2018b. Determination of correction factors in beta radiation beams using Monte Carlo method. Appl. Radiat. Isot. 140, 50–54.

Polo, I.O., Souza, W.S., Caldas, L.V.E., 2019. Monte Carlo approach for the determination of the angular dependence of an extrapolation chamber response. Encontro de Outono da Sociedade Brasileira de Física (EOSBF). Aracaju, SE, Brazil. https://sec.sbfisica.org.br/eventos/eosbf/2019/programa.

PTB, 2005a. Physikalisch-Technische Bundesanstalt. Calibration Certificate of $^{85}$Kr Source. PTB-6.34-BSS2_04. Braunschweig.

PTB, 2005b. Physikalisch-Technische Bundesanstalt. Calibration Certificate of $^{147}$Pm Source. PTB-6.34-BSS2_04. Braunschweig.

PTB, 2005c. Physikalisch-Technische Bundesanstalt. Calibration Certificate of $^{90}$Sr + $^{90}$Y source.PTB-6.34-BSS2_04. Braunschweig.

PTW, 2002. Physikalisch-Technische Werkstätten. Instruction Manual – Extrapolation Chamber according to Böhm, Type 23392. Freiburg: PTW.

Reynaldo, S.R., 2015. Characterization of an Extrapolation Chamber as a Primary Standard for Absorbed Dose Measurements in Beta Radiation Fields. Ph.D. Thesis. Center for the Development of Nuclear Technology, CDTN /CNEN, Belo Horizonte, Brazil (In Portuguese).

Selvam, P.T., SaulL, P.R.B., Rogers, D.W.O., 2005. Monte Carlo modelling of the response of NRC's $^{90}$Sr/$^{90}$Y primary beta standard. Med. Phys. 32, 3084–3094.

Vahabi, S.M., Zafarghandi, M.S., Ghasemi, M., Alipoor, A., Shahvar, A., 2014. A prototype of an extrapolation chamber for beta radiation beams of $^{90}$Sr + $^{90}$Y. J. Radioanal. Nucl. Chem. 301, 91–96.

Zoros, E., Pappas, E., Pantelis, E., 2014. Evaluation of the accuracy of the electron transport algorithms of the MCNP6 and EGSnrc Monte Carlo codes using the Fano theorem. Phys. Med. 30 (1), e113.